

University of Groningen

## Strategy for Enhancing the Dielectric Constant of Organic Semiconductors Without Sacrificing Charge Carrier Mobility and Solubility

Torabi, Solmaz; Jahani, Fatemeh; Van Severen, Ineke; Kanimozhi, Catherine; Patil, Satish; Havenith, Remco W. A.; Chiechi, R.C.; Lutsen, Laurence; Vanderzande, Dirk J. M.; Cleij, Thomas J.

*Published in:*  
Advanced Functional Materials

*DOI:*  
[10.1002/adfm.201402244](https://doi.org/10.1002/adfm.201402244)

**IMPORTANT NOTE:** You are advised to consult the publisher's version (publisher's PDF) if you wish to cite from it. Please check the document version below.

*Document Version*  
Final author's version (accepted by publisher, after peer review)

*Publication date:*  
2015

[Link to publication in University of Groningen/UMCG research database](#)

### *Citation for published version (APA):*

Torabi, S., Jahani, F., Van Severen, I., Kanimozhi, C., Patil, S., Havenith, R. W. A., Chiechi, R. C., Lutsen, L., Vanderzande, D. J. M., Cleij, T. J., Hummelen, J. C., & Koster, L. J. A. (2015). Strategy for Enhancing the Dielectric Constant of Organic Semiconductors Without Sacrificing Charge Carrier Mobility and Solubility. *Advanced Functional Materials*, 25(1), 150-157. <https://doi.org/10.1002/adfm.201402244>

### **Copyright**

Other than for strictly personal use, it is not permitted to download or to forward/distribute the text or part of it without the consent of the author(s) and/or copyright holder(s), unless the work is under an open content license (like Creative Commons).

### **Take-down policy**

If you believe that this document breaches copyright please contact us providing details, and we will remove access to the work immediately and investigate your claim.

*Downloaded from the University of Groningen/UMCG research database (Pure): <http://www.rug.nl/research/portal>. For technical reasons the number of authors shown on this cover page is limited to 10 maximum.*

DOI: 10.1002/ ((please add manuscript number))

**Article type: Full Paper**

**Strategy for Enhancing the Dielectric Constant of Organic Semiconductors Without Sacrificing Charge Carrier Mobility and Solubility**

*Solmaz Torabi, Fatemeh Jahani, Ineke Van Severen, Catherine Kanimozhi, Satish Patil, Remco W. A. Havenith, Ryan C. Chiechi, Laurence Lutsen, Dirk J. M. Vanderzande, Thomas J. Cleij, Jan C. Hummelen and L. Jan Anton Koster\**

S. Torabi, F. Jahani, Dr. R. C. Chiechi, Dr. R. W. A. Havenith, Prof. J. C. Hummelen, Dr. L. J. A. Koster  
Zernike Institute for Advanced Materials  
University of Groningen  
Nijenborgh 4, 9747 AG Groningen, The Netherlands  
E-mail: [l.j.a.koster@rug.nl](mailto:l.j.a.koster@rug.nl)

F. Jahani, Dr. R. C. Chiechi, Dr. R. W. A. Havenith, Prof. J. C. Hummelen  
Stratingh Institute for Chemistry,  
University of Groningen  
Nijenborgh 4, 9747 AG Groningen, The Netherlands

Dr. I. Van Severen, Prof. T. J. Cleij, Prof. D. Vanderzande  
Institute for Materials Research (IMO)  
Hasselt University  
Martelarenlaan 42, 3500 Hasselt, Belgium

C. Kanimozhi, Prof. S. Patil  
Solid State and Structural Chemistry Unit  
Indian Institute of Science  
560012, Bangalore, India

Dr. R. W. A. Havenith  
Ghent Quantum Chemistry Group  
Department of Inorganic and Physical Chemistry  
Ghent University  
Krijgslaan 281 (S3), B-9000 Ghent, Belgium

Dr. L. Lutsen, Prof. D. Vanderzande  
IMEC, IMOMEC Associated Laboratory  
Wetenschapspark 1, Diepenbeek, Belgium

Prof. T. J. Cleij  
Maastricht Science Programme  
Maastricht University  
P.O. Box 616, 6200 MD Maastricht, the Netherlands

Keywords: charge transport, conjugated polymers, fullerene derivatives, organic electronics, structure-property relationships

**Abstract:** Current organic semiconductors for organic photovoltaics (OPV) have relative dielectric constants (relative permittivities,  $\epsilon_r$ ) in the range of 2-4. As a consequence, coulombically bound electron-hole pairs (excitons) are produced upon absorption of light, giving rise to limited power conversion efficiencies. We introduce a strategy to enhance  $\epsilon_r$  of well-known donors and acceptors without breaking conjugation, degrading charge carrier mobility or altering the transport gap. The ability of ethylene glycol (EG) repeating units to rapidly reorient their dipoles with the charge redistributions in the environment was proven via density functional theory (DFT) calculations. Fullerene derivatives functionalized with triethylene glycol side chains were studied for the enhancement of  $\epsilon_r$  together with poly(*p*-phenylene vinylene) and diketopyrrolopyrrole based polymers functionalized with similar side chains. The polymers showed a doubling of  $\epsilon_r$  with respect to their reference polymers in identical backbone. Fullerene derivatives presented enhancements up to 6 compared with phenyl-C<sub>61</sub>-butyric acid methyl ester (PCBM) as the reference. Importantly, the applied modifications did not affect the mobility of electrons and holes and provided excellent solubility in common organic solvents.

## 1. Introduction

Organic semiconductors, thanks to their versatility, promise for larger scale, lower cost and easier production of electronic devices as compared to their inorganic counterparts. Upon growing demands for renewable energy, the photovoltaic application of organic semiconductors has received a great deal of attention over the past few decades. To realize large scale commercialization, the power conversion efficiency is one of the most important features that should be improved for organic photovoltaics (OPV). In contrast to inorganic photovoltaics where the absorption of light leads to the formation of free charge carriers, in OPV excitons (bound electron and hole pairs) are created upon excitation by light. This is

mainly due to the low dielectric constant of current OPV materials where electrons and holes cannot overcome their binding energy, which exceeds the thermal energy at room temperature. Taking this fact into account, bulk heterojunction (BHJ) solar cells were designed in which exciton dissociation is facilitated at the interface of so called donor-acceptor materials bearing favorable ionization potential-electron affinity for exciton dissociation.<sup>[1-2]</sup> Upon the introduction of the BHJ concept, a turning point was achieved in the progress map of OPV followed by impressive efficiency enhancements approaching to the values over 10%. This improvement has been achieved due to the vast amount of research dedicated to morphology, band structure and device design optimization. Nevertheless, the dielectric constant enhancement of organic materials captured less attention in these optimization efforts, which demands more research being devoted to this issue.

In a simulation study, Koster *et al.*<sup>[3]</sup> have predicted efficiencies of more than 20% by taking an increased relative dielectric constant (relative permittivity,  $\epsilon_r$ ) up to 10 into account. The enhancement of  $\epsilon_r$  up to frequencies of GHz can diminish loss processes in OPV devices originating from coulomb interactions between oppositely charged carriers as follows:

a) Bimolecular recombination is reversely proportional to  $\epsilon_r$  and occurs within  $\sim\mu\text{s}$  timescale.<sup>[4]</sup> An increased  $\epsilon_r$  in the  $\sim\text{MHz}$  range, therefore, leads to a reduced bimolecular recombination rate hence improved charge carrier extraction. The reduced bimolecular recombination enables the production of OPV devices with thicker films for better light harvesting.<sup>[5]</sup> Moreover, the thicker films will be favorable for upscaling the OPV technology for printing processes. b) Increasing  $\epsilon_r$  up to  $\sim\text{GHz}$  range can lead to a reduced exciton binding energy regarding exciton lifetime ( $\sim 10^{-9}$  s).<sup>[6]</sup> c) The lifetime of the charge transfer exciton is in  $\sim\text{ns}$  time domain.<sup>[7-8]</sup> A better screening for the charge transfer state can result from increased  $\epsilon_r$ .<sup>[9-10]</sup> d) The increased  $\epsilon_r$  reduces the singlet-triplet energy splitting which allows for smaller band offsets without relaxation to the triplet state.<sup>[11]</sup> The smaller band offset leads to the increased open circuit voltage. To sum up, an enhancement of  $\epsilon_r$  in the GHz

range is adequate to address the major loss factors of the photocurrent originating from coulomb interactions considering the timescale of the loss processes.

In optimized OPV cells ~100% internal quantum efficiency has been reported<sup>[12]</sup> however, it is worth noting that a significant open circuit voltage loss as a direct consequence of the band offset between the donor and acceptor compounds is still required for current low dielectric constant OPV materials. Moreover, the recombination in optimized BHJ systems is minimized at the cost of the reduced thickness of the active layer, hence the loss of light absorption efficiency.<sup>[5]</sup>

Therefore, tailoring organic materials for enhanced  $\epsilon_r$  is a viable route for efficiency enhancement of current OPV systems while potentially benefiting other applications of organic semiconductors that currently suffer from their poor dielectric properties. In a more ambitious perspective, the enhancement of  $\epsilon_r$  for organic materials can rule out the need for the BHJ structures upon a reduction of the exciton binding energy, directing the progressive pathway of OPV to a new milestone.

To date, only very few attempts at increasing the dielectric constant of organic semiconductors have been published.<sup>[13-16]</sup> Non-synthetic approaches such as physically mixing organic semiconductors with high- $\epsilon_r$  molecules or ion doping seem to be straightforward yet less likely to keep the absorption, transport and morphology unaffected. In a recent study, the physical addition of known high- $\epsilon_r$  molecules to a donor material has led to a reduced exciton binding energy, at the cost of significantly lower mobility and absorption.<sup>[15]</sup> Ion doping, another approach, can lead to an undesirable phase separated morphology of the donor-acceptor network.<sup>[16]</sup> In addition, ionic polarizations are not fast enough to screen coulomb forces even within the timescale of the slowest loss processes such as bimolecular recombination. Breselge *et al*<sup>[13]</sup> introduced triethylene glycol (TEG) side chains in a poly(*p*-phenylene vinylene) (PPV) derivative and showed an enhancement of  $\epsilon_r$ . When blended with a fullerene derivative, this polymer yielded enhanced charge dissociation as compared with a

less polar PPV derivatives.<sup>[14]</sup> However, the BHJ solar cell did not present efficiency enhancement reportedly due to the incompatible polarities of the donor and acceptor leading to the formation of large domains in the donor-acceptor network.<sup>[13]</sup> Therefore, in order to provide better mixing for the donor-acceptor blend it is beneficial to functionalize both components with identical polarities. Moreover, when the whole medium consists of donors/acceptors with enhanced  $\epsilon_r$ , loss processes arising from coulomb interaction become unfavorable.

Here we enhance  $\epsilon_r$  of both fullerene derivatives and conjugated polymers through compatible functionalization approaches. For this purpose, we choose to use pendant groups bearing higher polarities without modifying the  $\pi$ -conjugated system, so as not to affect the mobility or band gap. The dipoles in these pendant groups should be able to freely rotate even at relatively high frequencies ( $\sim$ GHz). We show that ethylene glycol repeating units fit these criteria and yield high dielectric constant organic semiconductors.

## 2. Materials

The nomenclature used in this manuscript is as following: EG=ethylene glycol, TEG= chains consisting two or three ethylene glycol repeating units.

Molecular dynamic studies on poly(ethylene glycol) (PEG) have confirmed their high chain flexibility and rapid motion of polar components.<sup>[17]</sup> EG and TEG yield  $\epsilon_r$  values in the range of 5-40 in the liquid phase at drive frequencies of 1-20 GHz.<sup>[18]</sup> According to density functional theory (DFT) calculations (B3LYP/6-31G\*\*) applied for a model TEG chain (**Figure 1**), using GAMESS-UK<sup>[19]</sup>, rotation around the H<sub>2</sub>C-CH<sub>2</sub> and H<sub>2</sub>C-O bonds can be very fast at room temperature. The rotational profiles (**Table S1**) around these bonds show two low barriers of  $\sim$ 0.11 and  $\sim$ 0.08 eV for H<sub>2</sub>C-CH<sub>2</sub> and H<sub>2</sub>C-O rotations and larger barriers of  $\sim$ 0.35 and  $\sim$ 0.29 eV respectively (**Figure 2a**). The activation energy of 0.11 eV corresponds to a reaction rate of  $0.95 \times 10^9 \text{ s}^{-1}$  at 175K according to equation 1.<sup>[20]</sup>

$$k_{rate} = \frac{k_b T}{h} \exp\left(-\frac{\Delta G}{RT}\right) \quad (1)$$

where  $k_{rate}$  is the reaction rate,  $k_b$ ,  $h$  and  $R$  are Boltzmann, Planck and gas constants respectively,  $T$  is the temperature and  $\Delta G$  is the Gibbs free energy difference. Thus the rotation of angles  $\phi$  between  $\sim 75^\circ$  and  $\sim 285^\circ$  of all bonds at low temperatures occurs readily. Full rotation is still active at 175K to overcome the barrier of 0.35 eV. The reaction rates of  $1.7 \times 10^{11} \text{ s}^{-1}$  and  $1.7 \times 10^7 \text{ s}^{-1}$  correspond to the activation energies of 0.11 eV and 0.35 eV respectively at 298K. Hence, at room temperature, rotations of  $\phi$  between  $\sim 75^\circ$  and  $\sim 285^\circ$  are active in GHz frequency-domain and full rotation in MHz range occurs readily. During these rotations, the magnitude of the dipole moment barely changes, but the direction of this dipole moment changes considerably (Figure 2b,c).

The swiftness and flexibility of TEG chains can provide easier reorientations for dipole moments, and thus potentially increase  $\epsilon_r$  when being added to donors or acceptors in the GHz range. The water solubility of EGs is another advantage which brings about new possibilities towards water processable OPV.

To follow the effect of EG side chains on the dielectric constant of three important OPV materials, a set of fullerene derivatives and polymers functionalized with TEG side chains were studied (**Figure 3**). Fullerene derivatives are known as the most efficient acceptors in OPV and show excellent electron transport properties.<sup>[21]</sup> In order to enhance the dielectric constant, TEG side chains were added to  $C_{60}$ , to obtain the fullerene derivatives PTEG-1 and PTEG-2 (Figure 3 c,d).<sup>[22]</sup> To differentiate the role of TEG on the dielectric constant of fullerene derivatives, an analogous fullerene derivative (PP) without TEG side chains (Figure 3 b) was synthesized.<sup>[22]</sup> The influence of TEG side chains was studied for diketopyrrolopyrrole (DPP) and PPV based polymers as well. The former shows very good ambipolar transport yielding field effect mobility exceeding  $10^{-2} \text{ cm}^2 \text{ V}^{-1} \text{ s}^{-1}$ .<sup>[23]</sup> It also has an absorption spectrum extending to the near infrared region. The latter lies in a well-studied

class of polymers for a wide range of electronic applications.<sup>[24]</sup> 2DPP-OD-OD, the studied DPP based polymer, was used as the reference compound for 2DPP-OD-TEG in which two of the side chains of the monomer were TEG substituted (Figure 3 e,f). Poly[2-methoxy-5-(2-ethylhexyloxy)-1,4-phenylenevinylene] (MEH-PPV) was used as the reference compound for PEO-PPV in which 2-ethylhexyloxy side chain is replaced with TEG (figure g,h). The synthetic routes to prepare PTEG-1, PTEG-2 and PP are reported in the reference 22. The synthetic routes of TEG functionalized DPP and PPV based polymers are published in references 23 and 13 respectively.

### 3. Determination of the relative dielectric constant

A conventional experimental method to determine  $\epsilon_r$  of solids is the parallel-plate-capacitance measurement with impedance spectroscopy. The material sandwiched between two metallic parallel electrodes is subject to a small perturbation of low amplitude AC signal with sweeping frequency usually from MHz range to tenths of Hz. The obtained impedance response is used to extract the capacitance value from

$$C^* = \frac{1}{j\omega Z^*} = \frac{-Z''}{\omega|Z|^2} + j \frac{-Z'}{\omega|Z|^2} \quad (2)$$

where  $j^2 = -1$  and  $Z^*$  is defined as the impedance complex function indicating impedance value at a particular frequency. The dielectric function can then be derived from

$$\epsilon_r^*(\omega) = \frac{C^*(\omega)}{C_0} = \epsilon'_r - j\epsilon''_r \quad (3)$$

where  $C_0 = \epsilon_0 A/d$  is the capacitance of the empty capacitor,  $\epsilon_0 = 8.85 \times 10^{-12} \text{ Fm}^{-1}$  is the electric permittivity of vacuum,  $A$  is the area of the material sandwiched between the electrodes and  $d$  is its thickness. The real part of the dielectric function corresponds to the relative dielectric constant,  $\epsilon_r$ , of the material under test and the imaginary part encompasses loss mechanisms such as conductance and relaxation processes. In a real capacitor however, the measured impedance comprises the response of the all circuit elements such as contacts, junctions and



feed lines. Therefore, employing a proper equivalent circuit model in which resistive or inductive effects are assigned to individual circuit elements can provide a fixed value corresponding to the capacitance through fitting over the experimental data. Nonetheless, not in all cases the capacitance response is merely associated with the dielectric properties of the bulk. In particular semiconductors, due to their certain degree of conductance, need a careful impedance measurement approach for the determination of  $\epsilon_r$ .

The capacitance response of organic semiconductors can be influenced by the accumulation of space charge filling the bulk and interfacial trap states,<sup>[25-26]</sup> recombination processes<sup>[27]</sup> or purely conductive behavior of the bulk. Biasing the device reversely up to an extent that the active layer is almost entirely depleted from charge carriers can help the capacitance response to converge into the geometrical value  $C_g = \epsilon_0 \epsilon_r A/d$ . In the presence of ionic contributions (dopants) though, the application of a reverse bias is not helpful to decouple bulk response from ionic polarizations.<sup>[28]</sup> A substantial increase in the capacitance at lower frequencies is indicative of ionic contributions, since ions are too slow to influence higher frequency impedance response.

Computational and experimental studies<sup>[29-30]</sup> on organic films indicate that their capacitance response is dependent on the selection of the contacts as well. For instance once the film is sandwiched between two Ohmic contacts with zero built-in voltage ( $V_{bi}$ ), no specific bias voltage at which the capacitance value converges to  $C_g$  is applicable. In contrast, once the film is sandwiched between two Ohmic contacts with non-zero built-in voltage, at  $V < V_{bi}$  capacitance converges to  $C_g$ . Regarding injection issue, therefore, applying steady voltages well below  $V_{bi}$  can keep the charge carriers away from being injected into the device.

In this work we chose to use indium-tin-oxide (ITO) covered with poly (3,4-ethylenedioxythiophene):poly(styrenesulfonic acid) (PEDOT:PSS) as anode. All devices were tested for current–voltage characteristics to roughly estimate  $V_{bi}$ . Then we applied an AC harmonic of 10mV in the frequency range of 100 Hz to 1MHz superimposed on a negative

DC bias to the capacitor and obtained the impedance response to find  $C_g$ . We applied several DC biases ( $V < V_{bi}$ ) to make sure the capacitance response is not dependent on biasing. In a separate experiment we used bare ITO as anode to make sure the presence of PEDOT:PSS does not influence the results. Apart from a higher standard deviation around average values, the magnitude of the relative dielectric constant found from capacitors using bare ITO did not differ from those with PEDOT:PSS included. Comparison of their current-voltage characteristics revealed that the films spun on bare ITO bottom electrode have higher leakage current at reverse bias which accounts for higher degree of error they impose on the measurements arising from the roughness of ITO. The absence of space charge polarization effects which are extrinsic to the material's dielectric properties was verified upon testing several capacitors in different film thicknesses. For each film thickness four capacitors varying in their electrode area ( $0.095 \text{ cm}^2$ ,  $0.1616 \text{ cm}^2$ ,  $0.357 \text{ cm}^2$ ,  $0.995 \text{ cm}^2$ ) were defined as a standard layout. All measured data presented perfect linear dependence of the capacitance with respect to the contact area which confirmed geometry independence of the results.

#### 4. Determination of the mobility

The determination of the charge carrier mobility is a crucial characterization step in organic electronics. For polymer/fullerene OPV devices, fullerene derivatives and polymers are recognized as electron and hole transporting medium respectively. To determine the mobility of electrons/holes of fullerenes/polymers in a solar cell structure, the space charge limited current (SCLC) method was chosen. In the case of a Poole-Frenkel type mobility, the SCLC is given by<sup>[31]</sup>

$$J_{SCL} = \frac{9}{8} \epsilon_0 \epsilon_r \mu(T) \exp(0.89\gamma(T)) \sqrt{\frac{V_{int}}{L}} \frac{V_{int}^2}{L^3} \quad (4)$$

where  $J_{SCL}$  is the electron (hole) current density,  $\mu$  is zero field mobility of the electrons (holes),  $\gamma$  is an empirical parameter describing the field activation which depends on the

temperature,  $V_{\text{int}}$  is the internal voltage (applied voltage corrected for  $V_{\text{bi}}$  and voltage drop through the series resistance of the connections) and  $L$  is the thickness of the active layer.

We designed single carrier devices by employing proper electrodes that can inject only electrons for fullerene derivatives and holes for polymers to study charge carrier mobility. By measuring current density versus voltage at different temperatures and fitting the results with equation 4, we could find SCL mobility values of each material together with their temperature dependence. For typical charge concentrations in organic semiconductors, the charge carrier mobility exhibits an Arrhenius temperature dependence.<sup>[31]</sup>

$$\mu = \mu_{\infty} \exp(-\Delta / kT) \quad (5)$$

where  $\mu_{\infty}$  is a universal value for the mobility and  $\Delta$  is the activation energy. We found the activation energy from equation 5 using the temperature dependent mobility values for each compound.

## 5. Results and discussions

**Table 1** lists  $\epsilon_r$  values of all test materials determined via IS in the frequency range of 100Hz to 1MHz. The equivalent circuit of **Figure 4** depicts the circuit elements that modeled the impedance response of all tested samples with estimated error of less than 1% (**Figure S1**). The relative dielectric constant of tested materials were calculated from dividing the fitted capacitance value to  $C_0$ . To resolve the effectiveness of the functionalization of donors and acceptors with EG side chains, they were studied comparatively to their reference chemical structures, differing only in their side chains. PTEG-1 and PTEG-2 presented relative dielectric constants up to  $\sim 6$  while PCBM as a widely used acceptor in OPV and PP as the reference compound yielded  $\epsilon_r \sim 4$ . Likewise, the TEG-functionalized polymers were compared to their reference polymer with identical backbone, but with hydrocarbon side chains. PEO-PPV proved  $\epsilon_r$  enhanced to  $\sim 6$  in comparison to its reference polymer MEH-PPV with  $\epsilon_r \sim 3$ . 2DPP-OD-TEG also showed the enhancement of  $\epsilon_r$  to a value more than twice as 2DPP-OD-OD with  $\epsilon_r \sim 2$ . In general, the fast change in the direction of the dipole

moment can account for the high  $\epsilon_r$  of materials with incorporated ethylene glycol chains. **Figure 5** depicts  $\epsilon_r$  versus frequency calculated by equation 3 while the series resistance of the contacts was subtracted from  $Z^*(\omega)$ . As can be seen,  $\epsilon_r$  is weakly dependent on the frequency, which means that the obtained values are attributed to the polarization mechanisms of the materials rather than space charge polarizations or ionic movements. However, 2DPP-OD-TEG shows frequency dependence at frequencies below 10kHz which might be due to the presence of ionic contributions. Nevertheless, ionic polarizations are less probable to remain active at frequencies higher than 10kHz where the value of  $\epsilon_r$  is still higher than that of the reference compound evident from Figure 5b. As is clear from the DFT calculations in section 2, the reaction rate for the change in the dipole moment direction is strongly temperature dependent for a model TEG chain. Speculated from these calculations the temperature dependence of  $\epsilon_r$  was studied for TEG-functionalized compounds. As can be seen from **Figure 6**,  $\epsilon_r$  of PEO-PPV and PTEG-2 is temperature dependent. However the temperature dependence for 2DPP-OD-TEG and PTEG-1 is not detectable similar to their reference compound. This might be due to the presence of steric effects in the solid state and different molecular packing of each compound that can influence the dipole moment alignments.

The enhancements of  $\epsilon_r$  were confirmed by the measurements up to frequencies of MHz which can effectively diminish bimolecular recombination rate. Referring to the literature values<sup>[18]</sup> and our DFT calculations, one may not expect a drop of  $\epsilon_r$  values at frequencies from 1MHz up to GHz range (at room temperature). Therefore, enhancement of  $\epsilon_r$  is likely to contribute in diminishing the loss processes occurring in the time domain of *ns* as discussed in section 1.

The electron mobilities of PTEG-1 and PTEG-2 were determined to be  $2 \times 10^{-7} \text{ m}^2 \text{V}^{-1} \text{s}^{-1}$  and  $3.5 \times 10^{-7} \text{ m}^2 \text{V}^{-1} \text{s}^{-1}$  respectively with the apparent activation energy of  $\sim 0.2 \text{ eV}$  (**Figure 7 a,b**) which are similar to that of PCBM ( $\mu_{\text{e-PCBM}} = 2 \times 10^{-7} \text{ m}^2 \text{V}^{-1} \text{s}^{-1}$ ,  $E_{\text{act-PCBM}} \sim 0.2 \text{ eV}$ ).<sup>[32]</sup> For 2DPP-OD-TEG polymer the study of SCL transport yielded mobility values for both electrons and

holes as  $2 \times 10^{-8} \text{ m}^2 \text{V}^{-1} \text{s}^{-1}$  with activation energy of 0.2 eV (Figure 7 d,c). These values are consistent with the results reported elsewhere.<sup>[33]</sup> **Figure 8** depicts the Arrhenius plot of obtained mobilities for extraction of the activation energy. An earlier study of the hole transport in PEO-PPV also retrieved a similar value for the hole mobility as MEH-PPV ( $\mu_{\text{h-MEH-PPV}} = 1.4 \times 10^{-10} \text{ m}^2 \text{V}^{-1} \text{s}^{-1}$ ).<sup>[34,14]</sup> The absence of hysteresis in the current-voltage characteristics and the quadratic dependence of the current to the voltage indicate a trap-free SCLC for the tested compounds.

## 6. Conclusion

In this work the relative dielectric constants of conjugated polymers and fullerene derivatives, previously restricted to the range of  $\sim 2$ -4, were boosted to the range of  $\sim 5$  to  $\sim 6$  via functionalization with highly polar EG side chains. Such enhancement was realized without breaking conjugation, degrading charge carrier transport, introduction of trap states and reducing solubility. Since loss processes originating from coulomb interactions between oppositely charge carriers are not beyond the *ns* timescale, therefore the applied strategy is an effective neat method for tailoring organic compounds for a higher  $\epsilon_r$  in the frequency range up to GHz. Additional to their great potential in enhancing the performance of OPV devices through increased  $\epsilon_r$ , the studied fullerene derivatives and polymers can provide desirable morphologies in BHJ donor/acceptor network owing to a higher miscibility resulting from their compatible polarities. In addition, the hydrophilic character of TEG side chains, can open up new possibilities for solution processing from renewable solvents as a long term impact for tailoring state of the art organic materials.

## 7. Experimental section

*Device fabrication:* Commercially available glass substrates patterned with ITO in four different dimensions ( $0.095 \text{ cm}^2$ ,  $0.1616 \text{ cm}^2$ ,  $0.357 \text{ cm}^2$ ,  $0.995 \text{ cm}^2$ ) were used to function as bottom electrode for capacitors. The substrates were cleaned by soap/water solution scrubbing, de-ionized water flushing, sonication with acetone and isopropyl alcohol followed by oven

drying and UV-OZONE treatment. PEDOT:PSS (VP AI4083, H.C. Starck) was spin cast in ambient conditions and oven dried at 140 °C for 10 minutes. All films (fullerene derivatives or polymers) were spun from chloroform under N<sub>2</sub> atmosphere. Metallic top contacts including interlayers (LiF(1nm), Ba (5nm), MoO<sub>3</sub> (10nm)) were deposited at a pressure of  $\sim 10^{-6}$  mbar with thermal evaporation.

*Device Characterization:* Impedance spectroscopy was performed in the range of 100 Hz to 1 MHz using a Solartron 1260 impedance gain-phase analyzer with an AC drive voltage of 10 mV. Current-voltage characterization was conducted with Keithley 2400 source meter. All measurements were performed in N<sub>2</sub> at stable temperature.

### **Acknowledgements**

L.J.A.K. acknowledges support by a grant from STW/NWO (VENI 11166). The work by S.T. and F.J.B. is part of the research program of the Foundation for Fundamental Research on Matter (FOM), which is part of the Netherlands Organization for Scientific Research (NWO). This is a publication by the FOM Focus Group 'Next Generation Organic Photovoltaics', participating in the Dutch Institute for Fundamental Energy Research (DIFFER).

## References

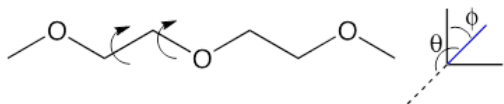
- [1] G. Yu, J. Gao, J. C. Hummelen, F. Wudl, A. J. Heeger, *Science*. **1995**, 270, 1789.
- [2] J. J. M. Halls, C. A. Walsh, N. C. Greenham, E. A. Marseglia, R. H. Friend, S. C. Moratti, A. B. Holmes, *Nature*. **1995**, 376, 498.
- [3] L. J. A. Koster, S. E. Shaheen, J. C. Hummelen, *Adv. Energy Mater.* **2012**, 2, 1246.
- [4] J. Guo, H. Ohkita, H. Benten, S. Ito, *J. Am. Chem. Soc.* **2010**, 132, 6154.
- [5] M. Lenes, L. J. A. Koster, V. D. Mihailetschi, P. W. M. Blom *Appl. Phys. Lett.* **2006**, 88, 243502.
- [6] J.-W. van der Horst, P. A. Bobbert, P. H. L. de Jong, M. A. J. Michels, L. D. A. Siebbeles, J. M. Warman, G. H. Gelinck, G. Brocks, *Chem. Phys. Lett.* **2001**, 334, 303.
- [7] J. H. Choi, K.-I. Son, T. Kim, K. Kim, K. Ohkubo, S. Fukuzumi, *J. Mater. Chem.* **2010**, 20, 475.
- [8] D. Veldman, Ö. Ipek, S. C. J. Meskers, J. Sweelssen, M. M. Koetse, S. C. Veenstra, J. M. Kroon, S. S. van Bavel, J. Loos, R. a J. Janssen, *J. Am. Chem. Soc.* **2008**, 130, 7721.
- [9] M. a. Loi, S. Toffanin, M. Muccini, M. Forster, U. Scherf, M. Scharber, *Adv. Funct. Mater.* **2007**, 17, 2111.
- [10] B. Bernardo, D. Cheyns, B. Verreet, R. D. Schaller, B. P. Rand, N. C. Giebink, *Nat. Commun.* **2014**, 5, 3245.
- [11] A. Köhler , H. Bässler , *J. Mater. Chem.* **2011** , 21 , 4003.
- [12] S. H. Park, A. Roy, S. Beaupr é, S. Cho, N. Coates, J. S. Moon, D. Moses, M. Leclerc, K. Lee, A. J. Heeger, *Nat Photonics*. **2009**, 3, 297.
- [13] M. Breselge, I. Van Severen, L. Lutsen, P. Adriaenssens, J. Manca, D. Vanderzande, T. Cleij, *Thin Solid Films*. **2006**, 511, 328.
- [14] M. Lenes, F. B. Kooistra, J. C. Hummelen, I. Van Severen, L. Lutsen, D. Vanderzande, T. J. Cleij, P. W. M. Blom, *J. Appl. Phys.* **2008**, 104, 114517.

- [15] S. Y. Leblebici, T. L. Chen, P. Olalde-Velasco, W. Yang, B. Ma, *ACS Appl. Mater. Interfaces*. **2013**, *5*, 10105.
- [16] X. Liu, K. S. Jeong, B. P. Williams, K. Vakhshouri, C. Guo, K. Han, E. D. Gomez, Q. Wang, J. B. Asbury, *J. Phys. Chem. B* **2013**, *117*, 15866.
- [17] R. J. Sengwa, *Polym. Int.* **1998**, *45*, 43.
- [18] R. Sengwa, K. Kaur, R. Chaudhary, *Polym. Int.* **2000**, *49*, 599.
- [19] M. F. Guest, I. J. Bush, H. J. J. van Dam, P. Sherwood, J. M. H. Thomas, J. H. van Lenthe, R.W.A. Havenith, J. Kendrick, *Mol. Phys.* **2005**, *103*, 719
- [20] F. Jensen, *Introduction to Computational Chemistry, 2nd edition*, John Wiley & Sons, Ltd, UK Chichester, **2007**, Ch. 13.
- [21] D. F. Kronholm, J. C. Hummelen, A. B. Sieval, P. Van't Hof (Solenne BV), *NL*. **8435713**, **2013**
- [22] F. Jahani, S. Torabi, R. C. Chiechi, L. J. A. Koster, J. C. Hummelen, (Submitted for Publication)
- [23] C. Kanimozhi, N. Yaacobi-Gross, K. W. Chou, A. Amassian, T. D. Anthopoulos, S. Patil, *J. Am. Chem. Soc.* **2012**, *134*, 16532.
- [24] M. Pope, C. E. Swenberg, *Electronic Processes in Organic Crystals and Polymers*, Oxford University Press, NY USA, 1999
- [25] E. Knapp, B. Ruhstaller, *J. Appl. Phys.* **2012**, *112*, 024519.
- [26] J. Bisquert, G. Garcia-Belmonte, Á. Pitarch, H. J. Bolink, *Chem. Phys. Lett.* **2006**, *422*, 184.
- [27] E. Ehrenfreund, C. Lungenschmied, G. Dennler, H. Neugebauer, N. S. Sariciftci, *Appl. Phys. Lett.* **2007**, *91*, 012112.
- [28] V. Shrotriya, Y. Yang, *J. Appl. Phys.* **2005**, *97*, 054504.
- [29] S. L. M. van Mensfoort, R. Coehoorn, *Phys. Rev. Lett.* **2008**, *100*, 086802.
- [30] F. Liu, P. P. Ruden, I. H. Campbell, D. L. Smith, *Appl. Phys. Lett.* **2012**, *101*, 023501.

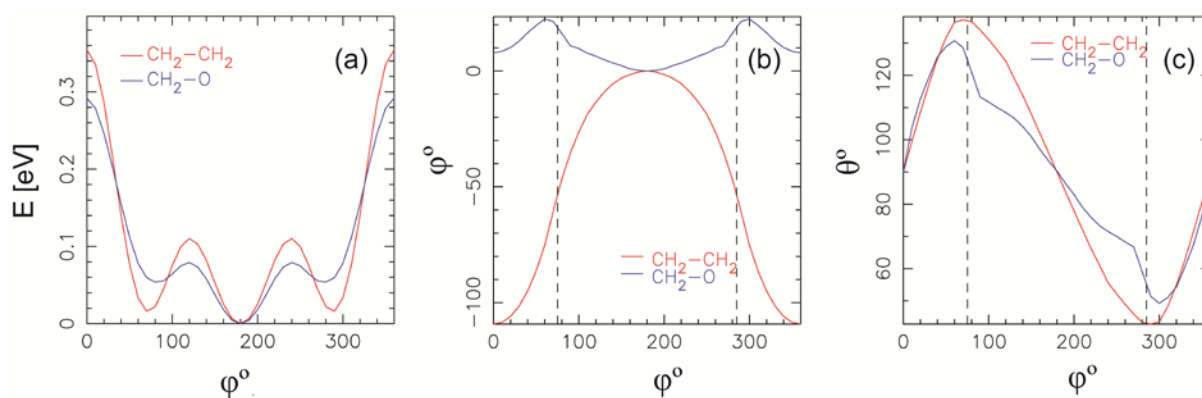


- [31] P. N. Murgatroyd, *J Phys D: Appl Phys.* **1970**, *3*, 151.
- [32] N. Craciun, J. Wildeman, P. Blom, *Phys. Rev. Lett.* **2008**, *100*, 056601.
- [33] Satyaprasad P. Senanayak, A. Z. Ashar, Catherine Kanimozhi, Satish Patil, K. S. Narayan, (Submitted for Publication).
- [34] Y. Zhang, B. de Boer, P. W. M. Blom, *Phys. Rev. B* **2010**, *81*, 085201.

**Figure 1.** Repeating units of EG. Indicated are the rotations around the  $\text{H}_2\text{C-CH}_2$  and  $\text{H}_2\text{C-O}$  bonds, and the axes of the direction of the dipole moment with respect to the molecule ( $\theta$ ,  $\phi$ ).



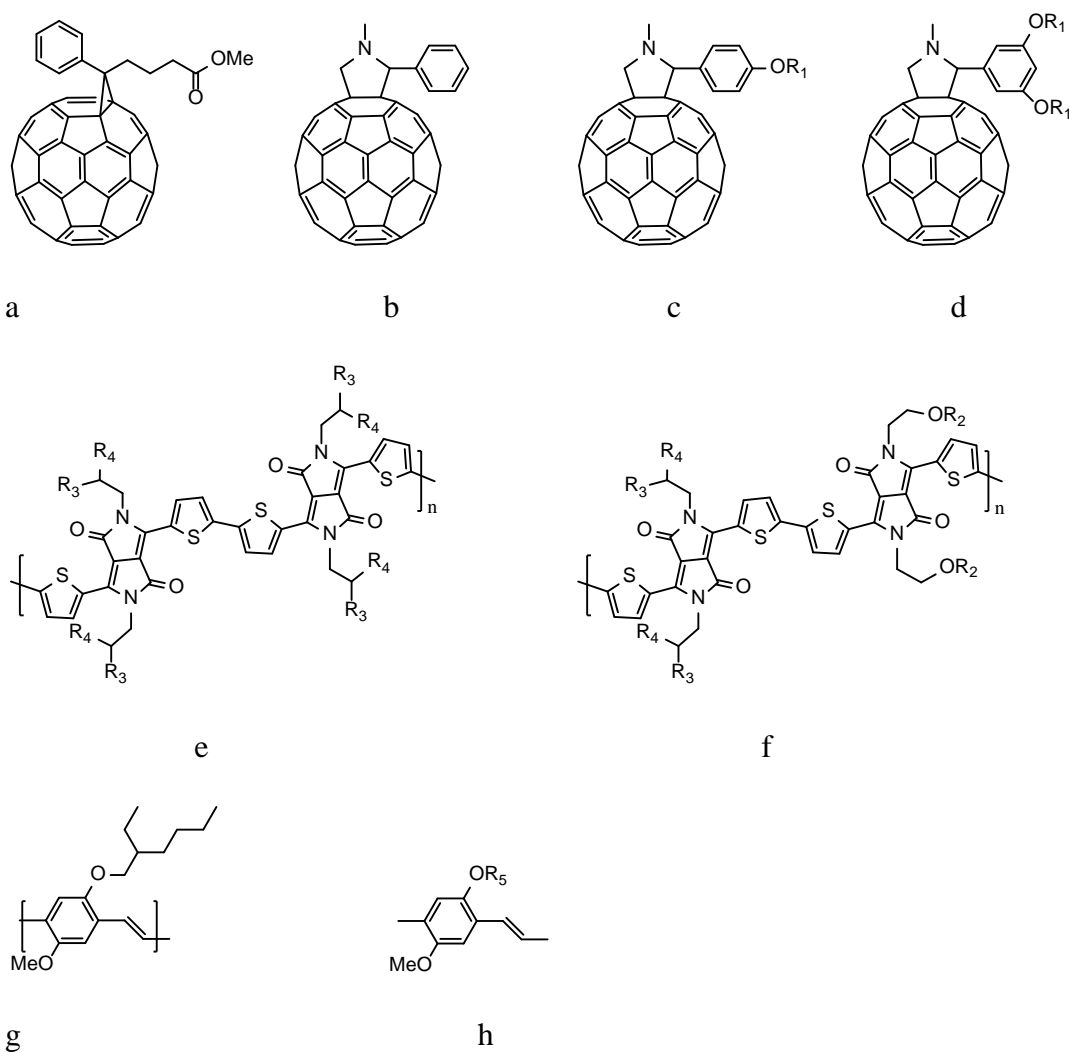
**Figure 2.** a) The energy with respect to the minimum as a function of the dihedral angle of the  $\text{H}_2\text{C-CH}_2$  and  $\text{H}_2\text{C-O}$  bonds, b) the angle  $\theta$  of the dipole moment as a function of the dihedral angle of the  $\text{H}_2\text{C-CH}_2$  and  $\text{H}_2\text{C-O}$  bonds, and c) the angle  $\phi$  of the dipole moment as a function of the dihedral angle of the  $\text{H}_2\text{C-CH}_2$  and  $\text{H}_2\text{C-O}$  bonds.

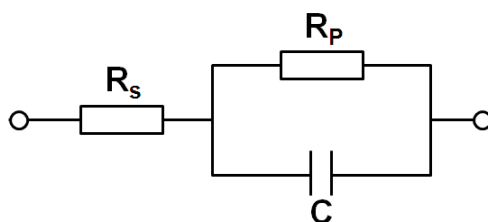


**Figure 3.** Chemical structures of fullerene derivatives and polymers functionalized for enhancement of  $\varepsilon_r$  and their reference compounds.

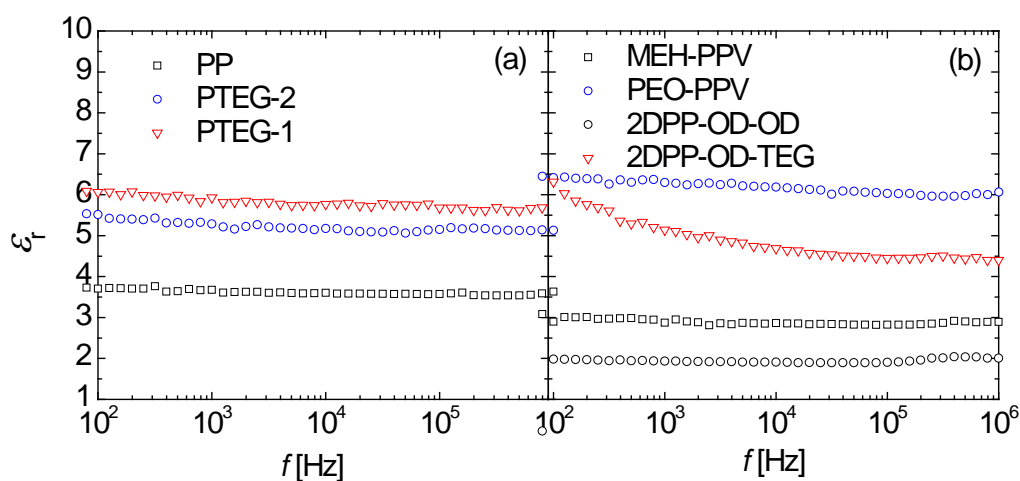
a) Phenyl- $C_{61}$ -butyric acid methyl ester (PCBM), b) PP c) PTEG-1 d) PTEG-2 e) 2DPP-OD-OD f) 2DPP-OD-TEG g) poly[2-methoxy-5-(2-ethylhexyloxy)-1,4-phenylenevinylene], h) PEO-PPV.

$R_1=(CH_2CH_2O)_3CH_2CH_3$ ,  $R_2=(CH_2CH_2O)_2CH_3$ ,  $R_3=C_8H_{17}$ ,  $R_4=C_{10}H_{21}$ ,  $R_5=(CH_2CH_2O)_3CH_3$



**Figure 4.** Equivalent circuit applied to model the experimental capacitance behavior.**Table 1.** The relative dielectric constant of fullerene derivatives and polymers

<i>Fullerene derivatives</i>	$\epsilon_r$	<i>tested capacitors #</i>
PP	$3.6 \pm 0.4$	8
PTEG-1	$5.7 \pm 0.2$	6
PTEG-2	$5.3 \pm 0.2$	16
PCBM	$3.9 \pm 0.1$	8
<i>Polymers</i>	$\epsilon_r$	<i>tested capacitors #</i>
2DPP-OD-TEG	$4.8 \pm 0.1$	10
2DPP-OD-OD	$2.1 \pm 0.1$	8
PEO-PPV	$6 \pm 0.1$	20
MEH-PPV	$3 \pm 0.1$	12

**Figure 5.** The relative dielectric constant of tested fullerene derivatives (a) and polymers (b) versus frequency.

**Figure 6.** Temperature dependence of the relative dielectric constant. a) PTEG-1 and PTEG-2 compared with PCBM b) 2DPP-OD-TEG and PEO-PPV compared with MEH-PPV. The lines are guides to the eye.

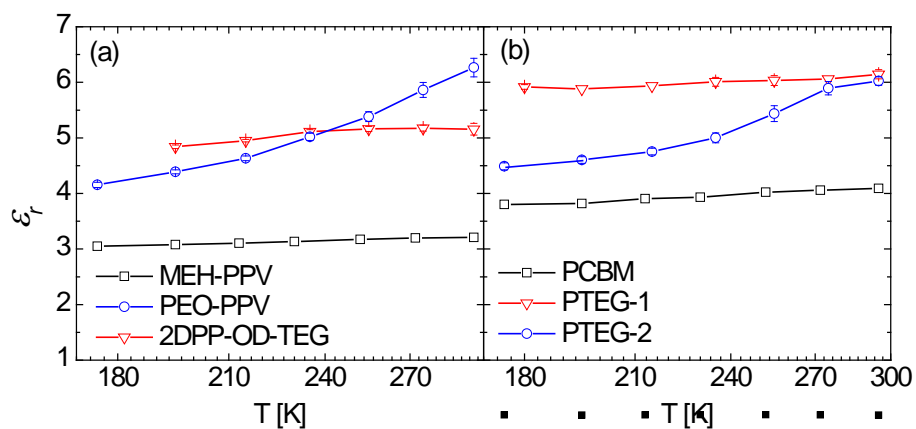


**Figure 7.** Steady state current voltage corrected for  $V_{bi}$  of a) Al/PTEG-2(192nm)/Al, b) Au/PEDOT:PSS/PTEG-1(145nm)/LiF/Al, d) Al/2DPP-OD-TEG(80nm)/Ba/Al electron-only devices and c) Au/PEDOT:PSS/2DPP-OD-TEG (96nm)/MoO<sub>3</sub>/Al hole-only device at temperatures ranging from 295K-215K in 20 K steps. Data (symbols) are fitted with equation 4 (lines). The gamma values ( $\gamma$  [V m<sup>-1</sup>]<sup>1/2</sup>) for each fit are provided in the legend.

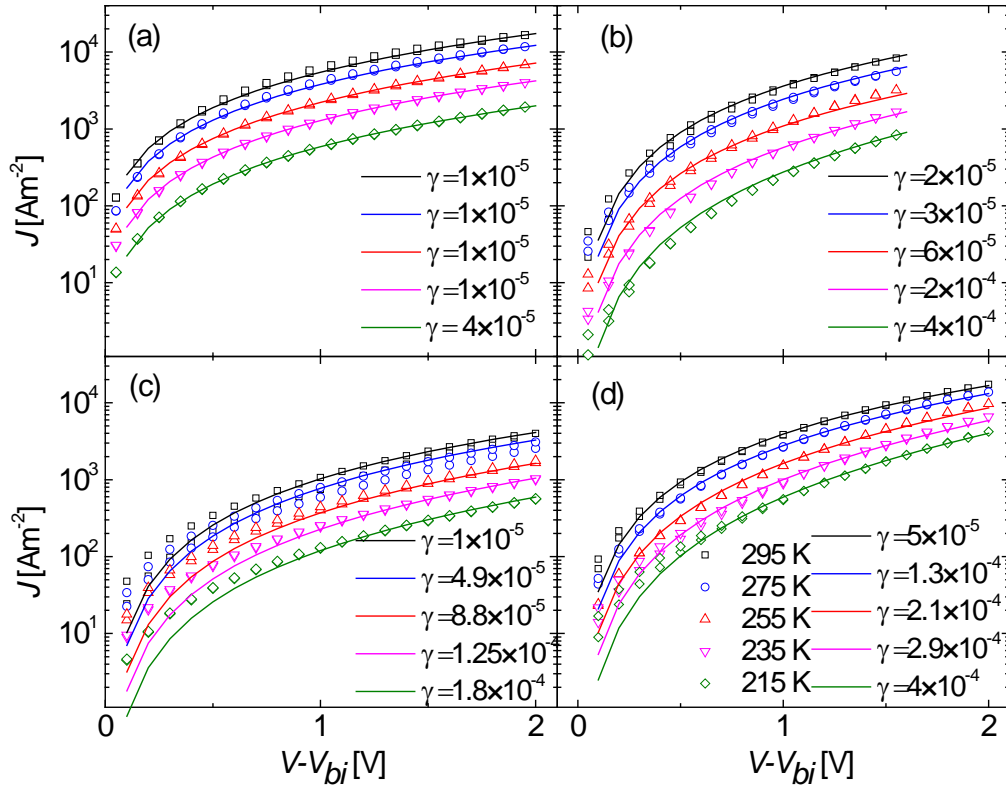
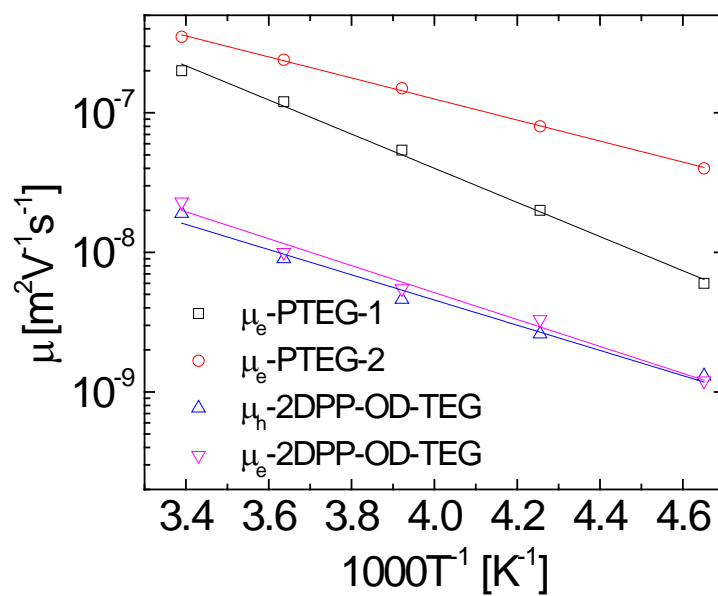


**Figure 8.** Mobility of charge carriers versus temperature for PTEG-2, PTEG-1 and 2DPP-OD-TEG (symbols) and corresponding Arrhenius fit (lines) yield the activation energies  $\sim 0.2$  eV.



A **synthetic strategy** is presented for the dielectric constant enhancement of organic semiconductors. It is demonstrated that fullerene derivatives, DPP and PPV based polymers show a marked increase of the relative dielectric constant when being functionalized with TEG side chains. Density functional theory calculations attribute such enhancements to the rapid reorientations of ethylene glycol dipoles on the side chains.

**Keyword** charge transport, conjugated polymers, fullerene derivatives, organic electronics, structure-property relationships

Solmaz Torabi, Fatemeh Jahani, Ineke Van Severen, Catherine Kanimozhi, Satish Patil, Remco W. A. Havenith, Ryan C. Chiechi, Laurence Lutsen, Dirk J.M. Vanderzande, Thomas J. Cleij, Jan C. Hummelen and L. Jan Anton Koster

### Strategy for Enhancing the Dielectric Constant of Organic Semiconductors Without Sacrificing Charge Carrier Mobility and Solubility

